

Correlations in the two-dimensional random-field Ising model

U. Glaus

Department of Physics and Astronomy, University of Maryland, College Park, Maryland 20742

(Received 28 April 1986)

Using transfer matrices, we calculate the connected and disconnected correlation functions of the random-field Ising model on long strips of width $N \leq 8$. The results, where extrapolated to the thermodynamic limit, are in good qualitative agreement with neutron scattering experiments of Birgeneau *et al.* [Phys. Rev. B **28**, 1438 (1983)] on the two-dimensional dilute Ising-like antiferromagnet $\text{Rb}_2\text{Co}_{0.7}\text{Mg}_{0.3}\text{F}_4$. For a particular probability distribution of the random field we propose that this model describes an adsorbed monolayer with a doubly degenerate ground state in the presence of frozen impurities and predict some features that could be detected with low-energy electron diffraction experiments on such systems. A modified mean-field theory gives a good qualitative account of the high-temperature behavior of the correlations of this model.

I. INTRODUCTION

Systems with quenched random impurities have been studied widely in the recent literature. This is partly due to the fact that real materials always contain a residual amount of defects that tends to disorder the crystalline structure in which they exist. One is therefore interested in describing the effect of impurities on the physical properties of such materials, in particular properties that are directly related to their ordered state.

On the other hand, the effect of randomness *per se* has also attracted a lot of attention; specifically in the context of phase transitions in systems with quenched disorder. While weak disorder in the interactions does not significantly alter the nature of the transition (at least in systems with a specific heat exponent $\alpha < 0$),¹ random fields that couple directly to the order parameter imply in general a drastically different critical behavior.

Both of the above-mentioned motivations have led us to investigate some properties of a specific model, namely the random-field Ising model (RFIM) in two dimensions (2D) defined by the Hamiltonian

$$H = -J \sum_{\langle ij \rangle} s_i s_j - \sum_i h_i s_i. \quad (1)$$

Here $s_i = \pm 1$ are Ising spins, J is the nearest-neighbor interaction strength, which will in the following be fixed at $J = 1$, and h_i is a random field satisfying $[h_i]_{\text{av}} = 0$, $[h_i h_j]_{\text{av}} = \delta_{ij}$, where $[\]_{\text{av}}$ denotes average with respect to the field distribution that will be specified later.

Although all current theoretical and experimental evidence states that, even for arbitrarily weak fields, the 2D RFIM will not undergo a phase transition, it nevertheless is of interest since the following two classes of systems are believed to be well described by this model.

(i) It has been pointed out by Fishman and Aharony² that a dilute Ising-like antiferromagnet in a uniform magnetic field is a realization of the RFIM. A neutron scattering study has subsequently been performed by Birgeneau *et al.*³ on the two-dimensional site-random Ising

antiferromagnet $\text{Rb}_2\text{Co}_{0.7}\text{Mg}_{0.3}\text{F}_4$ in varying uniform magnetic fields. We will qualitatively compare their structure-factor measurements to our calculations in Sec. III A, where we investigate Hamiltonian (1) with single-site probability distribution

$$p(h) = \frac{1}{2} [\delta(h + h_0) + \delta(h - h_0)] \quad (2a)$$

for the random field.

(ii) Systems of atoms chemisorbed on crystalline surfaces are usually modeled by lattice gases. Introducing random frozen impurities in order to model the fact that the substrate can have isolated defects that either strongly favor or prohibit adsorption, one is naturally led to a term

$$\sum_i h_i s_i$$

in the Ising transcription of the corresponding lattice-gas Hamiltonian. The distribution for the random field would then typically be

$$p(h) = \frac{p}{2} [\delta(h + h_0) + \delta(h - h_0)] + (1-p)\delta(h), \quad (2b)$$

where the density of defects $p \ll 1$ and the field strength $h_0 \gg 1$. Precisely such a distribution has also been proposed by Villain.⁴ In the limit $h_0 \rightarrow \infty$ this model can be easily solved exactly in one dimension.⁵ As h_0 is expected to be large, this limit should not affect the qualitative features of the system and we will report results on the $h_0 = \infty$ model in Sec. III B. Since low-energy electron diffraction (LEED) measurements are widely used in order to study such chemisorbed systems, it is of interest to have a qualitative picture of the structure factor for this particular distribution.

Due to the complexity of these systems theoretical results have been rather limited and were mostly concerned with bulk properties. Imry and Ma⁶ have put forward an argument based on the energy cost of flipping a domain of aligned spins immersed in a sea of spins with opposite sign that led them to conclude that the lower critical dimension d_c of the RFIM is equal to two. This argument

has later been improved by Chalker⁷ and Fisher *et al.*⁸ to include the entropy. It was also used as a starting point by Imbrie⁹ to prove the existence of long-range order in the 3D RFIM at $T=0$. The general consensus at present is therefore that the lower critical dimension of the RFIM is equal to two. This result is in conflict with the fact that the most divergent treelike Feynman graphs, generated in a perturbation expansion of the $\lambda\phi^4$ term in the Ginzburg-Landau version of the RFIM, are to all orders in λ equal to the ones of the ordinary Ising model with no random field in two dimensions less.¹⁰

Morgenstern *et al.*¹¹ have numerically computed thermodynamic quantities of the 2D RFIM with distribution (2a) on squares of sizes up to 12×12 with use of the transfer matrix. They also estimate the behavior of the spin-spin correlation function

$$[\langle s_0 s_l \rangle]_{av} \quad (3)$$

at low temperatures T and small fields h_0 by employing an approximate formula for the domain-wall density. In (3) the angular brackets denote the thermal average. Their result indicates that this correlation function decays exponentially with distance l of the spins from each other and a correlation length

$$\xi_{h_0} \underset{h_0 \rightarrow 0}{\sim} e^{(c/h_0^2)} \quad (T \ll 1). \quad (4)$$

This result is nicely consistent with predictions of other theories¹² based on the assumption that $d_c=2$. No theoretical (or numerical) attempt has so far been made to estimate the leading corrections to the exponential decay rate of (3) in the 2D RFIM. However, it is important to have such estimates in order to be able to compare them to the neutron scattering results of Birgeneau *et al.*³ and thereby test the validity of Hamiltonian (1) to describe these experiments. Mean-field theory based on the Ginzburg-Landau version of the RFIM predicts that the structure factor $S(q)$ [i.e., the Fourier transform of (3)] is given by

$$S(q) = \frac{\beta J}{q^2 + \xi^{-2}} + \frac{\beta^2 h_0^2}{(q^2 + \xi^{-2})^2}, \quad (5)$$

i.e., the sum of a Lorentzian (L) and a Lorentzian squared (L^2), resulting from the fact that $[\langle s_q \rangle \langle s_{-q} \rangle]_{av}$ is nonvanishing in the presence of a random field. This implies that the two-point correlation function (3) is equal to

$$\chi_{N,L}(q) = \frac{1}{NL} \sum_{n_1, l_1, n_2, l_2} e^{iq(l_1 - l_2)} [\langle s_{l_1 n_1} s_{l_2 n_2} \rangle - \langle s_{l_1 n_1} \rangle \langle s_{l_2 n_2} \rangle]_{av}, \quad (6)$$

where $q = 2\pi m/M$ and M is an integer factor of L and $0 \leq m \leq M-1$.

The "disconnected" part

$$D_{N,L}(q) = \frac{1}{NL} \left[\left| \sum_{n,l} e^{iq l} \langle s_{ln} \rangle \right|^2 \right]_{av} \quad (7)$$

$$[\langle s_0 s_l \rangle]_{av} = \left[\frac{A}{l^{(d-1)/2}} + \frac{B}{l^{(d-3)/2}} \right] e^{-(l/\xi)}.$$

In fact, the $L+L^2$ form has been extensively used by Birgeneau *et al.*³ to fit their neutron scattering data. The temperature and field strength dependence of the amplitudes in the mean field approximation can of course not be expected to give a reasonable approximation for the RFIM. Note however that the $L+L^2$ form for $S(q)$ is also obtained from the exact solution⁵ of the 1D RFIM with field distribution given by Eq. (2b) for $h_0 = \infty$ as well as from the exact solution of the random-field spherical model in all dimensions.¹³

In this paper, we report results of structure factor calculations of the RFIM on very long strips of width $N \leq 8$. For this purpose we use a slightly refined version of the modified transfer-matrix technique first employed by Morgenstern *et al.*¹¹ for this system and combine it with the method described by Droz and Malaspina¹⁴ for static-structure-factor calculations. We will shortly give the details of the calculations in the next section. We have preferred to use the transfer matrix method rather than the Monte Carlo method to avoid problems of equilibration.

In Sec. III A we report our results for the "weak" field distribution mentioned above and compare them to the neutron scattering experiment on $\text{Rb}_2\text{Co}_{0.7}\text{Mg}_{0.3}\text{F}_4$ in a uniform field. Section III B is devoted to the results obtained using the single field distribution (2b). Finally, we give our conclusions in Sec. IV. A detailed mean-field-theory calculation of $S(q)$ is presented in the Appendix starting with the Hubbard-transformed continuous-field version of the RFIM,¹⁵ and yielding more reasonable values than Eq. (5) for the amplitudes of L and L^2 at high temperatures.

II. METHOD FOR CALCULATING THE STRUCTURE FACTOR

We consider the RFIM on strips of width N in the y and length L in the x direction. Let the integer coordinates of the square lattice be labeled by (l, n) , $1 \leq l \leq L$, $1 \leq n \leq N$. We found it useful to divide the calculation for the structure factor into two parts. We only consider the wave-number dependence parallel to the x direction. We first calculated the susceptibility

was then calculated separately and hence the structure factor

$$S_{N,L}(q) = \frac{1}{NL} \sum_{l_1, n_1, l_2, n_2} e^{iq(l_1 - l_2)} [\langle s_{l_1 n_1} s_{l_2 n_2} \rangle]_{\text{av}} = \chi_{N,L}(q) + D_{N,L}(q), \quad (8)$$

which is measured in neutron scattering and LEED experiments. Following Ref. 14, we apply a q -dependent (non-random) magnetic field and therefore consider the total Hamiltonian:

$$H_\mu = \sum_{l=1}^L h_{l,l+1} + g_{\mu,l}, \quad (9a)$$

$$h_{l,l+1} = - \sum_{n=1}^N s_{l,n} s_{l+1,n}, \quad (9b)$$

$$g_{\mu,l} = - \sum_{n=1}^N s_{l,n} [s_{l,n+1} + h_{l,n} + \mu \cos(ql)]. \quad (9c)$$

Periodic boundary conditions are imposed in the y direction. Define the transfer matrix by

$$T_l^\mu = e^{-\beta g_{\mu,l}} e^{-\beta h_{l,l+1}}, \quad (10)$$

which acts on the 2^N -dimensional space V of spin configurations in row l ; note that the second factor in (10) is actually independent of l . A theorem due to Furstenberg¹⁶ guarantees then that starting with any vector v in V , the random-field average free energy per site $F_{\text{av}}^N(\mu)$ to the Hamiltonian (9a) is given by

$$F_{\text{av}}^N(\mu) = \lim_{L \rightarrow \infty} \left((-\beta LN)^{-1} \ln \left[\left\| \prod_{l=1}^L T_l^\mu v \right\| / \|v\| \right] \right), \quad (11)$$

where $\| \cdot \|$ denotes any vector norm in V . In other words, one need only consider one realization of the random-field distribution on a very long strip in order to perform field averages. Not much is known, unfortunately, about the rate of convergence in L but it appears to be well described by a power law for the temperatures we have considered.

We therefore find that

$$\chi_{N,L}(q) = \frac{\partial^2 F^{N,L}(\mu)}{\partial \mu^2} \Big|_{\mu=0} \quad (12)$$

is a self-averaging quantity, where $F^{N,L}(\mu)$ is given by the right-hand side of (11) before taking the limit.

In order to avoid taking the derivative in (12) numerically and thereby losing accuracy we have adopted the following procedure which seems to have been first used by Yeomans and Derrida.¹⁷ Since we are dealing with finite systems, $F^{N,L}(\mu)$ is an analytic function of μ and can be written in the form

$$F^{N,L}(\mu) = \frac{1}{L} \sum_{l=1}^L \ln Q_l^\mu, \quad (13)$$

where

$$Q_l^\mu = \|v_{l+1}\| / \|v_l\| \quad (14)$$

and $v_{l+1} = T_l v_l$. Expanding T_l and v_l in powers of μ ,

$$\begin{aligned} T_l &= T_l^{(0)} + \mu T_l^{(1)} + \mu^2 T_l^{(2)} + O(\mu^3), \\ v_l &= v_l^{(0)} + \mu v_l^{(1)} + \mu^2 v_l^{(2)} + O(\mu^3), \end{aligned} \quad (15)$$

and simultaneously iterating the three vectors $v_l^{(i)}$, one can express the coefficient in the expansion of Q_l^μ in powers of μ in terms of the $v_l^{(i)}$, $v_{l+1}^{(i)}$ and therefore obtain $\chi_{N,L}(q)$ without having to take any derivatives numerically. Using the technique of sparse matrices, the number of elementary arithmetic operations to be performed in order to obtain $\chi_{N,L}(q)$ is then proportional to $LN2^N$.

For the calculation of $D_{N,L}$ we first realize that, since the field distribution is uncorrelated between different sites, the probability distribution for the total field

$$H_{NL} = \sum_{n,l} h_{n,l} \quad (16)$$

approaches a Gaussian with variance proportional to $(NL)^{1/2}$. Therefore, for a given realization, the spins will be subjected to a net field of order $(NL)^{-1/2}$ per site and it is reasonable to assume that also the total magnetization $M = \sum_{l,n} \langle S_{ln} \rangle$ will be of order $(LN)^{1/2}$. Hence, $D_{N,L}(q)$ is not a self-averaging quantity and averages over several random field realizations have to be performed in order to obtain it. The error bars for $D_{N,L}(q)$ are then roughly estimated as

$$\frac{\Delta D_{N,L}(q)}{D_{N,L}(q)} \sim K^{-1/2}, \quad (17)$$

where K denotes the number of random-field configurations averaged over. For $q \neq 0$ the error (17) is reduced by an additional factor proportional to $q^{-1/2}$. We obtained $D_{N,L}(q)$ by applying, instead of the q -modulated external field $\mu \cos(ql)$, a magnetic field $\mu \delta_{l,l_0}$ separately on each row l_0 . We found that in order to obtain the local magnetization

$$\frac{1}{N} \sum_{n=1}^N \langle S_{l_0 n} \rangle = \frac{\partial F^{N,L}(\mu \delta_{l,l_0})}{\partial \mu} \Big|_{\mu=0} \quad (18)$$

we only had to iterate the transfer matrix ten rows beyond l_0 to obtain a 1% accuracy at the temperatures considered.

III. RESULTS FOR THE 2D RFIM

A. Binary single field distribution with $h_0 < 1$

Consider the Hamiltonian (1) with the single-site distribution (2a). With the susceptibility χ , we performed a simple test of the accuracy of our method using the result¹⁸

$$\left. \frac{\partial \chi_{N,L}(q=0)}{\partial \Delta} \right|_{\Delta=0} = -(\chi_{N,L}^0)^2, \quad (19)$$

where $\Delta = \beta^2 h_0^2$ and χ^0 is the pure (zero-field) susceptibility. Equation (19) holds for all temperatures in a finite system. In Table I we compare the two quantities in (19) for $T_c^0 = 2/\ln(\sqrt{2}+1)$, the transition temperature of the pure 2D Ising model. The derivative with respect to Δ was taken numerically. The error of χ/Δ seems to be less than 1% for $L = 2 \times 10^4$ at this temperature.

In Fig. 1, $\chi_{N,L}(q)$ is plotted against q for $T=2.5$, $h_0=0.5$, $N=5$, and $L=4 \times 10^4$. Also shown in Fig. 1 is the result of a fit of $\chi_{N,L}(q)$ to the form

$$\chi(q) = \frac{A}{(1+q^2\xi^2)} + \frac{B}{(1+q^2\xi^2)^2}, \quad (20)$$

with A , B , and ξ as fitting parameters. In the insert, we plot the resulting χ^2 of fits to the form (20) keeping the ratio of B/A fixed and fitting the remaining two parameters. Clearly, there is a sharp minimum at $B/A=0$ and it is seen in Fig. 1 that a pure Lorentzian accounts very well for the functional form of the q -dependent susceptibility. This result is somewhat unexpected in view of the expansion of the physical quantities in terms of powers of the random field used by Shapir and Aharony¹⁸ in order to obtain (19), which yields

$$\chi(q) = \chi^0(q) - \Delta[\chi^0(q)]^2 + O(\Delta^2). \quad (21)$$

It seems therefore that the higher order terms in Δ cancel the Lorentzian squared term obtained in first order.

The disconnected correlation function $D_{N,L}(q)$, defined in Eq. (7) is plotted in Fig. 2 for $T=2.35$, $h_0=0.5$, $N=5$, and $L=2000$, averaged over 50 realizations together with fits to a pure Lorentzian and Eq. (20). It is apparent that a fit to (20) with a predominantly Lorentzian-squared component accounts much better for the shape of $D_{N,L}(q)$ than a pure Lorentzian. Note also the noise in the data

TABLE I. Pure ($h_0=0$) system susceptibility χ^0 and derivative $(-\partial\chi/\partial\Delta|_{\Delta=0})^{-1/2}$ of the susceptibility χ with respect to $\Delta=(\beta h_0)^2$ at $\Delta=0$ and $\beta=\ln(\sqrt{2}+1)/2$ for $2 \leq n \leq 8$ and $L=2 \times 10^4$.

N	χ	$(-\partial\chi/\partial\Delta _{\Delta=0})^{-1/2}$
2	8.472	8.419
3	18.217	18.103
4	31.015	31.026
5	46.462	46.368
6	64.375	64.513
7	84.648	85.021
8	107.199	106.893

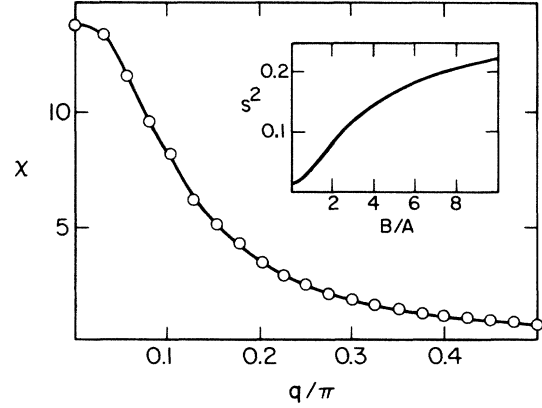


FIG. 1. Susceptibility χ vs q/π for $T=2.5$, $h_0=0.5$, $N=5$, and $L=4 \times 10^4$. The circles denote the numerical values. Solid line is best Lorentzian fit to χ . The inset shows least squared sum S^2 vs B/A of fits to Eq. (20) with constant B/A .

for small q due to the limited number of realizations averaged over. A simple mean field calculation (see Appendix) expected to be a reasonable approximation at high temperatures, yields

$$D(q) = \frac{B[g\beta \tanh(\beta h_0)]^2}{(1+\xi^2 q^2)^2}, \quad (22)$$

$$\xi^{-2} = 2d(1-2d\beta g), \quad g = 1 - \tanh^2(\beta h_0), \quad (23)$$

while $\chi(q)$ is given by

$$\chi(q) = g + \frac{gA\beta}{1+\xi^2 q^2}. \quad (24)$$

The constant g in (24) arises naturally in our mean field calculation and it comes from the fact that for Ising spins

$$\int dq \chi(q) = [\langle S_i^2 \rangle - \langle S_i \rangle^2]_{\text{av}} = 1 - [\langle S_i \rangle^2]_{\text{av}} \xrightarrow{\beta \rightarrow 0} 1. \quad (25)$$

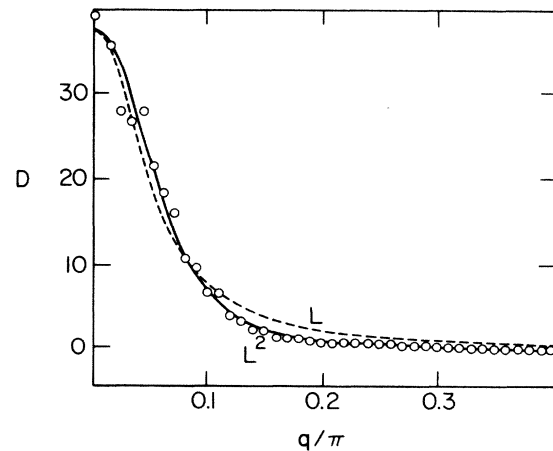


FIG. 2. Disconnected correlation function D vs q/π at $T=2.35$, $h_0=0.5$, $N=5$, and $L=2 \times 10^3$ averaged over 50 random-field realizations. Solid line denotes best fit to Eq. (21), which is a pure Lorentzian squared. Dashed line denotes best Lorentzian fit.

TABLE II. Correlation length's ξ_χ , obtained by fitting χ to a Lorentzian, and ξ_D , obtained by fitting D to a Lorentzian squared, for various temperatures and $3 \leq N \leq 7$. Error bars were obtained from variance of 20 independent runs for $N = 3$ and are expected to be the same for all N .

N	T					
	1.8		2.5		3.5	
	ξ_χ	ξ_D	ξ_χ	ξ_D	ξ_χ	ξ_D
3	4.3 ± 0.2	4.0 ± 0.3	2.15 ± 0.1	2.4 ± 0.2	1.24 ± 0.05	1.3 ± 0.1
4	5.4	5.0	2.6	2.6	1.35	1.20
5	6.7	5.6	2.8	3.1	1.32	1.35
6	8.5	6.0	3.0	3.1		
7	9.3	6.1	3.0	3.0		

Figure 1 shows that g is small for $T = 2.5$, but it clearly becomes appreciable for higher temperatures. In Table II, we list the correlation lengths ξ_χ and ξ_D for $h_0 = 0.5$ obtained from the fits of χ and D to the form (24) and (22), respectively. At temperatures above the pure system's transition temperature, ξ_χ and ξ_D agree within the errors, while at lower temperatures ξ_D is systematically smaller than ξ_χ . It is also apparent that at lower temperatures the Lorentzian squared form is no longer appropriate to describe $D(q)$ (Fig. 3).

We are now ready to compare our results to the measurements of Birgeneau *et al.*³ performed on the two-dimensional dilute Ising antiferromagnet $\text{Rb}_2\text{Co}_{0.7}\text{Mg}_{0.3}\text{F}_4$ in a uniform field. Such a comparison is necessarily qualitative, but we see no reason for the temperature dependence of the quantities measured to be significantly affected by the details of the probability distribution of the random field. A more severe limitation is the small width N of the strips, which allows a safe extrapolation to $N \rightarrow \infty$ only in cases where the bulk correlation length ξ is of the order of or less than the size of the largest strip. This forces us to exclude the low temperature, small random-field region where ξ becomes large. One could nevertheless perform a finite-size scaling analysis of the dependence of the correlation length on the random-field strength in this region in order to test the prediction in Eq. (4).

In the following, we identify the Néel temperature $T_N = 42.5$ K of the experiment with the critical tempera-

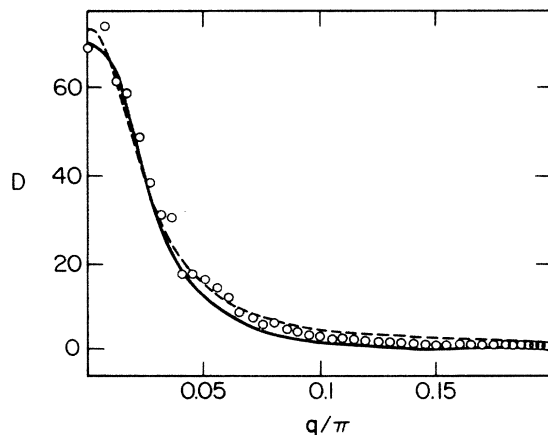


FIG. 3. Same as in Fig. 2 for $T = 1.3$, $h_0 = 0.5$, $N = 4$, and $L = 2 \times 10^3$ averaged over 200 random-field realizations.

ture T_c^0 of the IM in the absence of a random field, i.e., $T_c^0 \approx 2.269$. We first consider the correlation length ξ calculated from fitting $\chi(q)$ to a Lorentzian. In Fig. 4 we plotted the extrapolated inverse bulk correlation length versus temperature for $h_0 = 0.5$ and 0.75 . It is tempting to quantitatively compare this plot to Fig. 8 of Ref. 3, which would yield the conclusion that $h_0 = 0.5$ corresponds to a field strength $h \sim (35 \pm 3)$ kG for the uniform field applied in the experiment. Furthermore,

$$\xi_{\text{expt}} = (5.5 \pm 0.7) \xi_{\text{RFIM}},$$

where ξ_{expt} is the correlation length measured in lattice units (l.u.) by Birgeneau *et al.*³ and ξ_{RFIM} our estimate for the bulk correlation length (in l.u.) obtained with the transfer matrix method. Our results for ξ_{RFIM} are not affected by a finite-size effect in the considered region, as Monte Carlo simulations on square lattices of size 36×36 are in excellent agreement with our values.¹⁹ For $h_0 = 0.75$, extrapolations to the thermodynamic limit turned out to be possible even at low temperatures, where the correlation length becomes independent of temperature, as observed experimentally.

Next we compare the peak intensities, given in Fig. 2 of Ref. 3 to our estimates in Table III. Unfortunately, no accurate $N \rightarrow \infty$ extrapolation is possible at low temperatures, but the agreement is nevertheless satisfactory if we use the field strength correspondence obtained from com-

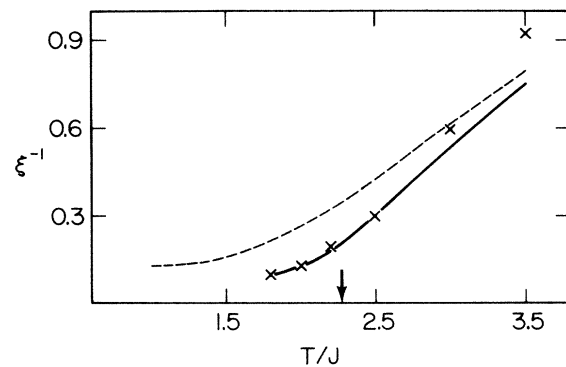


FIG. 4. Inverse correlation length ξ^{-1} (in l.u.) versus temperature for $h_0 = 0.5$ (solid line) and $h_0 = 0.75$ (dashed line). The crosses denote experimental values, adjusted as mentioned in the text, for $h = 35$ kG obtained by extrapolating between the 29.5-kG and the 40-kG curves in Fig. 8 of Ref. 3. Arrow indicates Ising model critical temperature T_c^0 .

TABLE III. Peak intensities $S(0)_{\text{RFIM}}$, determined numerically and extrapolated to $N \rightarrow \infty$, and $S(0)_{\text{expt}}$, measured experimentally, for various temperatures. $S(0)_{\text{expt}}$ was obtained by interpolating between the $h = 29.5$ kG and $h = 40$ kG curves of Fig. 2 of Ref. 3 and adjusted such that it agrees with $S(0)_{\text{RFIM}}$ at $T = 2.2$.

T	$S(0)_{\text{RFIM}}$	$S(0)_{\text{expt}}$
1.8	220 ± 40	284
2.0	150 ± 20	162
2.2	81 ± 10	81
2.35	57 ± 7	49
2.5	31 ± 3	24

paring the correlation lengths. A more significant comparison can be made by plotting the fractional contribution of the Lorentzian squared to the total intensity of the structure factor, because its temperature dependence was found experimentally to be almost independent of the field strength. We plotted an extrapolated estimate of this quantity in Fig. 5. For $T \leq 2.0$ we had to fit directly to the structure factor because, as mentioned above, separate fits to $\chi(q)$ and $D(q)$ do not yield the same correlation length below this temperature. The ratio was easily extrapolated to the thermodynamic limit in the temperature range shown because the N dependence was rather weak. Agreement with experiment is good for this quantity

B. Results for the strong-field case

In this section we consider Hamiltonian (1) with the single field distribution (2b) in the limit $h_0 \rightarrow \infty$. In other words, spins are frozen in their up or down state with probability $(p/2) \ll 1$. Such a model is expected to describe adsorbed systems with doubly degenerate ground states in the presence of frozen impurities.⁴ More precisely, imagine the square lattice being divided into rectangular cells, each containing two neighboring sites. Each cell is required to contain one adsorbed atom, whose position within the cell i is described by an Ising spin $s_i = \pm 1$. The mutual repulsion between the adsorbed atoms can be

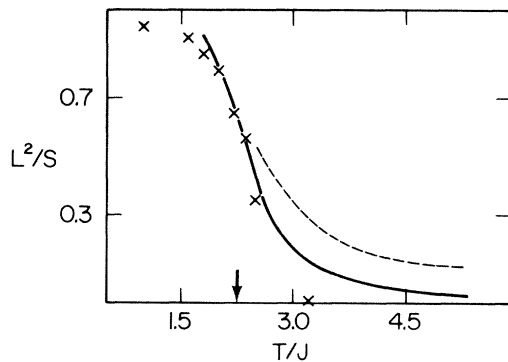


FIG. 5. Extrapolated estimate of the fractional contribution L^2/S of the Lorentzian squared term to the structure factor versus temperature for the RF distribution Eq. (2a) (solid line) and Eq. (2b) (dashed line). The crosses denote corresponding experimental values taken from Fig. 10 of Ref. 3. Arrow indicates T_c^0 .

described by an interaction equal to the one proposed in the Hamiltonian (1). Suppose that the impurities are randomly distributed over the lattice with a density $p/2$. For a given cell i , there is then a probability $p/2$ for an impurity to be located at each of the two sites described by the $s_i = \pm 1$ states for the Ising spin. Since it is energetically very unfavorable for an adsorbed atom to be located at the site of an impurity, the latter act like a random external field with distribution (2b) and $h_0 \gg 1$. It is somewhat artificial of course to require the adatoms to be distributed such that there is exactly one in each cell. If one did not require $[h_i]_{\text{av}} = 0$ for each site but rather $[h_i]_{\text{av}} = (-1)^{l+n}h$, where l and n denote the coordinate of site i in the lattice, this artificial restriction would be removed and the model would describe a lattice gas with nearest-neighbor repulsions in the presence of frozen impurities. The imposed restriction should be irrelevant for the qualitative behavior of the correlations described here. It should therefore be possible to observe the effects of such impurities on the structure factor by performing LEED experiments.

The exact solution of this model in one dimension (i.e., for $N = 1$) reveals that the structure factor is again given by the sum of a Lorentzian and a Lorentzian squared.⁵ In Fig. 6 we have plotted the fractional contribution L^2/S of the Lorentzian squared to the structure factor versus temperature for $p = 0.05$. Interestingly, this ratio has a maximum $L^2/S \approx 0.4$ at $T \approx 1$ and drops sharply toward zero for low temperatures. This behavior is in contrast to the experiment,³ where $S(q)$ was found to be predominantly Lorentzian squared even down to very low T . Unfortunately we cannot access the low-temperature region with our transfer matrix method, because the convergence becomes extremely slow there and extrapolations are impossible. It is therefore an open question whether Fig. 6 qualitatively describes the equilibrium behavior of the RFIM even in two dimensions and for more general single field distributions. We believe that this behavior could be due to the peculiar single field distribution in this case. In fact, for any $p > 0$, the 1D chain is broken into finite noninteracting pieces and it seems therefore natural to ex-

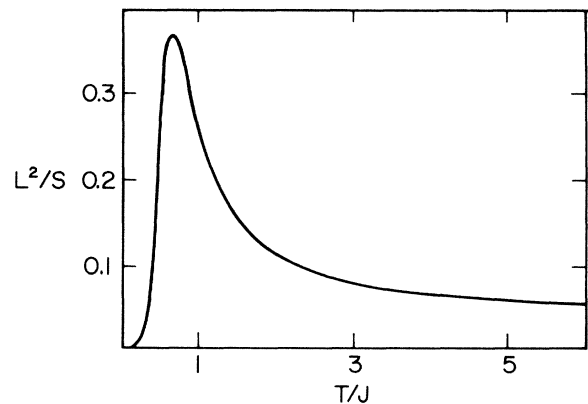


FIG. 6. Fractional contribution L^2/S of Lorentzian squared term to the structure factor versus temperature for the RF distribution Eq. (2b) for $h_0 = \infty$ and $N = 1$ (exact result from Ref. 5).

pect that similar behavior in 2D would only be observed if p is chosen to be larger than p_c , the critical probability for site percolation in two dimensions.

For higher temperatures, the behavior of L^2/S is in qualitative agreement with the one found in the previous Sec. III A. However, mean field theory (see Appendix) predicts an enhancement of L^2/S for the distribution (2b) compared to the one examined in Sec. III A. This enhancement is actually found from the transfer matrix results (see Fig. 5). $\chi(q)$ again is fitted excellently by a pure Lorentzian plus a constant while a Lorentzian squared accounts very well for $D(q)$. Moreover, excellent agreement is found between the correlation lengths obtained separately from χ and D only if one uses these functional forms for them.

In an experiment one should therefore be able to detect the following features related to the presence of frozen impurities.

(i) The transition is destroyed and with a sufficient resolution the correlation lengths should be seen to become independent of temperature at low T .

(ii) For wave vectors $k \lesssim 2\xi^{-1}$, the structure factor should be significantly better described by Eq. (20) than by a pure Lorentzian with a temperature dependence of the factors A and B that can be qualitatively inferred from Fig. 5.

IV. CONCLUSIONS

In this paper we have studied the RFIM on long strips using the modified transfer matrix technique to calculate static correlation functions. The statistical errors resulting from the finiteness of the strip length could be well controlled and did not pose a serious problem while the non-self-averaging property of the disconnected correlation function made extensive calculations necessary.

Since the purpose of this work is to compare calculated physical quantities to experiment we studied only the region in (T, h_0) plane, for which an extrapolation to the thermodynamic limit could be carried out safely; we double-checked our extrapolations with Monte Carlo results¹⁹ on large squares and found agreement in all cases. We first studied the “weak random field” case in Sec. III A using a binary distribution of strength $h_0 < J = 1$ for the field on a single site. At high temperatures $T \gtrsim T_c^0$, the transition temperature of the two-dimensional Ising model, the susceptibility $\chi(q)$ and the disconnected correlation function $D(q)$ are found to be well described by our modified mean field theory, while $D(q)$ starts to deviate from a pure L^2 for $T < T_c^0$, $\chi(q)$ is well described by a pure L for all temperatures considered. A detailed comparison to the neutron scattering experiments performed on the 2D dilute Ising-like antiferromagnet (AFM)

$\text{Rb}_2\text{Co}_{0.7}\text{Mg}_{0.3}\text{F}_4$ revealed that

(i) The temperature dependence of the correlation length of the RFIM for $h_0 = 0.5$ agrees quantitatively with the experiment provided we set

$$h = (35 \pm 3) \text{ kG} ,$$

$$\xi_{\text{expt}} = (5.5 \pm 0.7) \xi_{\text{RFIM}} ,$$

where h is the strength of the uniform field (note that we have put $J = 1$) and ξ_{expt} is the experimentally measured correlation length ξ_{RFIM} our calculated correlation length, in lattice units.

(ii) For $h_0 = 0.75$, we are able to extrapolate ξ_{RFIM} at temperatures sufficiently low to see that it actually becomes flat, in agreement with experiment.

(iii) Excellent agreement is found for the temperature dependence of the fractional ratio of the L^2 to the total intensity of the structure factor, which itself agrees reasonably well with experiment, provided we take the field strength found by comparing the correlation lengths.

While some of these results seem to agree fortuitously well with experiment considering the fact that we are comparing nonuniversal quantities, it seems safe to state that Hamiltonian (1) provides a very good description of the physics of the 2D dilute Ising AFM $\text{Rb}_2\text{Co}_{0.7}\text{Mg}_{0.3}\text{F}_4$. We believe therefore that we have provided significant support to the Fishman-Aharony mapping of dilute AFM's in a uniform field onto RFIM's.

In Sec. III B we reported results using the “strong field” distribution (2b) for the field on a single site. We first noticed the “dropoff” of the strength of L^2 at low temperatures obtained from the exact solution of this model in one dimension for $h_0 = \infty$. Since we cannot extrapolate our small strip results at these low temperatures, we cannot determine whether this dropoff is characteristic for the equilibrium behavior also in two dimensions at low temperatures, for a possible explanation see Sec. III B. The high-temperature behavior is qualitatively similar to that found in the weak field case, the amplitude of the L^2 being somewhat enhanced however; this result is also predicted by our modified mean field theory. If this model is appropriate to describe frozen impurities in adsorbed monolayers, it should be possible to detect the effects we described by performing LEED experiments on these systems.

ACKNOWLEDGMENTS

Useful discussions with N. C. Bartelt and T. L. Einstein are gratefully acknowledged. This research was supported by the Department of Energy under Grant No. DE-FG05-84ER45071.

APPENDIX: MEAN FIELD CALCULATION OF $S(q)$

We write the RFIM Hamiltonian as

$$H = - \frac{J}{2} \sum_{i,j} s_i (\Delta + 2d)_{ij} s_j - \sum_i [h_i + \mu \beta^{-1} \cos(qi)] s_i , \quad (\text{A1})$$

where Δ denotes the lattice Laplacian. Invoking the Hubbard transformation,

$$\exp\left[(\beta/2) \sum_{i,j} s_i A_{ij} s_j\right] = (\pi^n \det A)^{-1/2} \int_{-\infty}^{+\infty} \prod_{i=1}^n d\Psi_i \exp\left[-(2\beta J)^{-1} \sum_{i,j} \Psi_i A_{ij}^{-1} \Psi_j + \sum_i \Psi_i s_i\right], \quad (\text{A2})$$

where A_{ij} denotes any nonsingular $n \times n$ matrix and A_{ij}^{-1} its matrix inverse, the partition function for (A1), can be written as

$$Z = C \int_{-\infty}^{+\infty} \prod_i d\Psi_i \exp\left[-(2\beta J)^{-1} \sum_{i,j} \Psi_i (\Delta + 2d)_{ij}^{-1} \Psi_j + \sum_i \ln\{\cosh[\beta h_i + \mu \cos(qi) + \Psi_i]\}\right]. \quad (\text{A3})$$

The trace over the Ising spins produces the second sum in the exponential, which can be expanded in terms of increasing powers in the continuous field variables Ψ_i and the modulated external field $\mu \cos(qi)$.

$$\ln\{\cosh[\beta h_i + \mu \cos(qi) + \Psi_i]\} = \ln\{\cosh[\beta h_i + \mu \cos(qi)]\} + \tanh(\beta h_i) \Psi_i + [1 - \tanh^2(\beta h_i)][\mu \cos(qi) \Psi_i + \Psi_i^2]/2 + O(\Psi_i^3). \quad (\text{A4})$$

Neglecting the $O(\Psi_i^3)$ terms and performing the random-field average in the quadratic terms we arrive at the "mean-field" approximation

$$Z_{\text{MF}} = C \prod_i \cosh[\beta h_i + \mu \cos(qi)] \int_{-\infty}^{+\infty} \prod_i d\Psi_i \exp\left[-(2\beta J)^{-1} \sum_{i,j} \Psi_i A_{ij} \Psi_j + \sum_i [\tilde{h}_i + (g\mu/2) \cos(qi)] \Psi_i\right], \quad (\text{A5})$$

where

$$g = \int dh p(h) [1 - \tanh^2(\beta h)], \quad (\text{A5a})$$

$$\tilde{h}_i = \tanh(\beta h_i), \quad (\text{A5b})$$

$$A_{ij} = (\Delta + 2d)_{ij}^{-1} - \beta J g \delta_{ij}. \quad (\text{A5c})$$

Transforming the integral in (5) into momentum space and keeping only the two lowest order terms in the expansion of A_{ij} in terms of k^2 , we obtain

$$Z_{\text{MF}} = C \prod_i \cosh[\beta h_i + \mu \cos(qi)] \int_{-\infty}^{+\infty} \prod_k d\Psi_k \exp\left[\sum_k \left\{ \frac{k^2 + m^2}{8\beta J d^2} \Psi_k + \tilde{h}_k + \mu g \sqrt{N} \delta_{k,q} \right\} \Psi_{-k}\right] \quad (\text{A6})$$

where

$$m^2 = 2d(1 - 2d\beta J g). \quad (\text{A7})$$

Note that the equation $m^2 = 0$ is equivalent to the equation for the mean field phase transition found by Schneider and Pytte²⁰ and more generally by Aharony.¹⁵ Performing the Gaussian integral in (A6), the mean field approximation to the free energy is

$$-N\beta F_{\text{MF}}(\mu) = \sum_i \ln \cosh[\beta h_i + \mu \cos(qi)] - 4\beta J d^2 \sum_k \frac{(\tilde{h}_k + \mu g \sqrt{N} \delta_{k,q})^2}{k^2 + m^2}. \quad (\text{A8})$$

Therefore the averaged correlation functions are

$$[\langle s_q \rangle \langle s_{-q} \rangle]_{\text{av}}^{\text{MF}} = (8\beta J d^2 g)^2 \frac{[\tanh^2 \beta h]_{\text{av}}}{(q^2 + m^2)^2} \quad (\text{A9})$$

and

$$[\langle s_q s_{-q} \rangle - \langle s_q \rangle \langle s_{-q} \rangle]_{\text{av}}^{\text{MF}} = g + \frac{8\beta J d^2 g}{q^2 + m^2}. \quad (\text{A10})$$

Since the variance of the Gaussian integral (A6) is proportional to β , the low-order expansion in the fields Ψ_i performed in (A3) should become a good approximation at high temperatures. Furthermore, since in the quadratic terms the random field coefficient is replaced by its average, the variance of the random variables $\tanh(\beta h_i)$ should be small.

¹A. B. Harris, J. Phys. C 7, 1671 (1974).

²S. Fishman and A. Aharony, J. Phys. C 12, L729 (1979).

³R. J. Birgeneau, H. Yoshizawa, R. A. Cowley, G. Shirane, and H. Ikeda, Phys. Rev. B 28, 1438 (1983).

⁴J. Villain, J. Phys. (Paris) 43, L551 (1982).

⁵G. Grinstein and D. Mukamel, Phys. Rev. B 27, 4503 (1983).

⁶Y. Imry and S. K. Ma, Phys. Rev. Lett. 35, 1399 (1975).

⁷J. T. Chalker, J. Phys. C 16, 6615 (1983).

⁸D. Fisher, J. Frohlich, and T. Spencer, J. Stat. Phys. 34, 863 (1984).

⁹J. Z. Imbrie, Phys. Rev. Lett. 53, 1747 (1984); Commun. Math. Phys. 98, 145 (1985).

- ¹⁰G. Grinstein, Phys. Rev. Lett. **37**, 944 (1976); A. Aharony, Y. Imry, and S. K. Ma, *ibid.* **37**, 1367 (1976); A. P. Young, J. Phys. C **10**, L257 (1977); G. Parisi and N. Sourlas, Phys. Rev. Lett. **43**, 744 (1979).
- ¹¹I. Morgenstern, K. Binder, and R. M. Hornreich, Phys. Rev. B **23**, 287 (1980).
- ¹²A. Aharony and E. Pytte, Phys. Rev. B **27**, 5872 (1983); H. S. Kogon and D. J. Wallace, J. Phys. A **14**, L527 (1981).
- ¹³R. M. Hornreich and H. G. Schuster, Phys. Rev. B **26**, 3929 (1982).
- ¹⁴M. Droz and A. Malaspina, J. Phys. C **16**, L231 (1983).
- ¹⁵We follow closely the treatment of A. Aharony, Phys. Rev. B **18**, 3318 (1978).
- ¹⁶H. Furstenberg, Trans. Ann. Math. Soc. **68**, 377 (1963).
- ¹⁷J. Yeomans and B. Derrida, J. Phys. A **18**, 2343 (1985).
- ¹⁸Y. Shapir and A. Aharony, J. Phys. C **14**, L905 (1981).
- ¹⁹N. C. Bartelt (private communication).
- ²⁰T. Schneider and E. Pytte, Phys. Rev. B **15**, 1519 (1977).